

Los Alamos

NATIONAL LABORATORY

memorandum

Los Alamos Neutron Science Center, LANSCE-1
Accelerator Physics and Engineering Group

To: Distribution
From: Barbara Blind, LANSCE-1, H808
Robert Garnett, LANSCE-1, H817
Phone/Fax: 5-2607/5-2904
Symbol: LANSCE-1:99-181
Date: September 22, 1999
Email: bblind@lanl.gov

SUBJECT: Performance of Machines with Latest 14-Quadrupole SNS MEBT

Introduction

The latest SNS MEBT is a 14-quadrupole MEBT specified by John Staples from LBNL. It has a lot of engineering detail taken into account. Therefore, it has longer drifts between components than the previously specified 14-quadrupole MEBT [1]. At the same time, some apertures have changed. The 2.0-cm bore radii of the quadrupoles upstream of the chopper and downstream of the antichopper have been reduced to 1.5 cm. The 2.0-cm bore radii of the quadrupoles between chopper and antichopper have remained. The chopper and antichopper were changed from 0.50-m-long structures with 1.5-cm vertical apertures to 0.35-m-long structures with 1.8-cm vertical apertures. Instead of having to provide 20-mrad deflections, the chopper and antichopper only need to provide 16-mrad deflections.

This is a brief note to document two possible SNS MEBT foci, one for the LBNL RFQ output beams, provided by John Staples, and one for the LANL RFQ output beams. These RFQ output beams are described first. The MEBT was optimized using the respective no-errors RFQ output beam and in the simulations this focus was used for all corresponding with-errors RFQ output beams. A brief description of the performance of the whole machine with the latest SNS MEBT is also given. The requirement on the transverse rms emittances is met, both for the LBNL beams and the LANL beams.

LBNL RFQ Output Beams

John Staples provided us with eleven RFQ output beams. One was obtained by tracking 10,000 macroparticles through the RFQ without errors, the other ten were obtained by tracking 10,000 macroparticles through RFQs with errors. John considered a large number of errors of the RFQ input-beam parameters and the RFQ parameters. The RFQ input beam nominally had 60 mA of current, but one error considered was a fluctuation in the input-beam current.

The distributions obtained from LBNL contained the coordinates of all macroparticles, including those lost. The format used did not keep very many digits. The RFQ was simulated in the usual orientation. The latest MEBT, just like the earlier 14-quadrupole

MEBT, is designed for a beam from an RFQ that is rolled (rotated around the z axis) by 90° from this orientation.

Thus, we further processed the LBNL files by first removing the lost macroparticles from the distributions. To avoid possible problems with beams where many macroparticles have identical values for one of their coordinates, the coordinates were smeared out. For instance, a quantity written in f7.3 format had randomly added to it a number between -0.0005 and +0.0005. Finally, the particle distributions were rolled by 90°. This involved setting $x_{\text{new}}=y_{\text{old}}$, $x'_{\text{new}}=y'_{\text{old}}$, $y_{\text{new}}=-x_{\text{old}}$ and $y'_{\text{new}}=-x'_{\text{old}}$.

The input-beam currents of the eleven RFQs are shown in Table 1. Case 0 is the no-errors case, and cases 1 through 10 are the ten with-errors cases. Further, Table 1 gives the numbers of macroparticles transmitted through the RFQ and the RFQ output-beam currents. The average RFQ output-beam current of the ten with-errors beams is 51.9976 mA. It is also given in Table 1.

The no-errors RFQ output beam has 9160 particles and 54.96 mA of current. The Twiss parameters of the no-errors RFQ output beam, after the 90° roll, are $\alpha_x=-1.607$, $\beta_x=0.16012$ m, $\alpha_y=1.983$, $\beta_y=0.19556$ m, $\alpha_z=0.130$, $\beta_z=1.2828$ °/keV, as shown in Table 2. The emittances are $\epsilon_x=0.204$ π -mm-mrad, $\epsilon_y=0.206$ π -mm-mrad, $\epsilon_z=106.8$ π -°-keV, as shown in Table 3. The average phase is 1.368°. The phases range between -25.877° and 40.777°. The average beam energy is 2.507 MeV. The particle energies range between 2.470 MeV and 2.551 MeV. These values are shown in Table 4. The phases must be shifted appropriately before injection into the MEBT.

Table 2 also shows the Twiss parameters, and Table 3 shows the rms emittances, for the ten with-errors beams. Table 4 shows the average, minimum and maximum phase, and average, minimum and maximum energy for the ten with-errors beams.

The average Twiss parameters for the ten with-errors beams are $\alpha_x=-1.5489$, $\beta_x=0.152437$ m, $\alpha_y=1.8622$, $\beta_y=0.185474$ m, $\alpha_z=0.0051$, $\beta_z=1.12406$ °/keV, as shown in Table 2. The average rms emittances are $\epsilon_x=0.2250$ π -mm-mrad, $\epsilon_y=0.2262$ π -mm-mrad, $\epsilon_z=115.85$ π -°-keV, as shown in Table 3. There is a systematic difference between the no-errors case and all the with-errors cases.

LANL RFQ Output Beams

LANL also produced eleven RFQ output beams. One was obtained by tracking 10,000 macroparticles through the RFQ without errors, the other ten were obtained by tracking 10,000 macroparticles through RFQs with errors. There were considerably fewer RFQ errors than those considered by LBNL. Just like the LBNL distributions, the LANL distributions had to be rolled by 90°.

The input-beam currents for the ten RFQs with errors were 60 mA. The numbers of macroparticles transmitted through the RFQs, and the RFQ output-beam currents, are

shown in Table 5. The average RFQ output-beam current of the ten with-errors beams is 56.3994 mA.

The no-errors RFQ output beam has 9375 particles and 56.25 mA of current. The Twiss parameters of the no-errors beam, after the 90° roll, are $\alpha_x=-2.385$, $\beta_x=0.21317$ m, $\alpha_y=1.924$, $\beta_y=0.16708$ m, $\alpha_z=-0.170$, $\beta_z=1.2375$ °/keV, as shown in Table 6. The emittances are $\epsilon_x=0.187$ π -mm-mrad, $\epsilon_y=0.185$ π -mm-mrad, $\epsilon_z=104.6$ π -°-keV, as shown in Table 7. The average phase is -28.811° , with a range between -55.255° and 6.199° . The average beam energy is 2.507 MeV, with a range between 2.464 MeV and 2.555 MeV. These values are shown in Table 8.

Table 6 shows the Twiss parameters, and Table 7 shows the rms emittances, for the ten with-errors beams. Table 8 shows the average, minimum and maximum phase and average, minimum and maximum energy for the ten with-errors beams.

The average Twiss parameters for the ten with-errors beams are $\alpha_x=-2.3601$, $\beta_x=0.206069$ m, $\alpha_y=1.9098$, $\beta_y=0.161525$ m, $\alpha_z=-0.1622$, $\beta_z=1.1593$ °/keV, as shown in Table 6. The average rms emittances are $\epsilon_x=0.1894$ π -mm-mrad, $\epsilon_y=0.1898$ π -mm-mrad, $\epsilon_z=105.57$ π -°-keV, as shown in Table 7.

There again is a systematic difference between the no-errors case and the with-errors cases.

Comparison of LBNL and LANL RFQ Output Beams

LBNL considered many more RFQ errors than LANL and thus the LBNL RFQ output beams vary more from case to case. For instance, the LBNL beams have currents between 47.072 mA and 54.864 mA, while the LANL beams have currents between 55.614 mA and 57.216 mA. The average beam energies of all the with-errors beams are between 2.503 MeV and 2.522 MeV for the LBNL beams, and between 2.493 MeV and 2.496 MeV for the LANL beams. Since the energies of the LBNL beams are further from the nominal value, the bunching cavities do more harm to the beams. This is particularly obvious when following the development of the case-7 beam. Similarly, the phases occupy a larger range for the LBNL beams than for the LANL beams, again leading to bigger problems at the bunching cavities.

Figure 1 shows the phase distributions of the ten LBNL beams (top) and the ten LANL beams (bottom), and Figure 2 shows the energy distributions of the ten LBNL beams (top) and the ten LANL beams (bottom). Clearly the energy varies much less for the LANL beams than for the LBNL beams.

The RFQ will presumably be adjusted to deliver the correct beam energy and the bunching cavities will be rephased in response to the actual beam phase, so that using the same MEBT focus for all LBNL beams paints a pessimistic picture of the performance of the machine with the LBNL beams.

The various LBNL beams have a wider range of rms emittances than their LANL counterparts. The Twiss parameters are also somewhat different, but this was taken into account by establishing a different MEBT focus for the two sets of beams.

MEBT Foci

The center section of the MEBT is tuned to have a 180° zero-current phase advance between the center of the chopper and the center of the antichopper. The setting of the center quadrupoles was established with TRANSPORT.

We then adjusted the first four quadrupoles of the MEBT to achieve a beam with $\alpha_x=0.0$, $\beta_x=3.0$ m, $\alpha_y=0.0$, $\beta_y=0.7$ m at the midpoint of the center section. TRACE 3-D was used for this purpose. The TRACE 3-D input beam had the parameters of the no-errors RFQ output beam. Thus, the first four quadrupoles are set differently for the LBNL beams and the LANL beams.

We then adjusted the last four MEBT quadrupoles and the last MEBT cavity for a reasonable rms match to the DTL. It would have been better to have two cavities to accomplish the longitudinal match. However, the second cavity or the third cavity can not be used for this purpose, because it would affect the phase advance between the chopper and the antichopper. The first cavity can not be used because it would affect the focus at the chopper stopper. The optimization of the last four quadrupoles and the last cavity was done with PARMILA and TRACE 3-D, using the respective no-errors RFQ output beam.

The tunes for the MEBT with the LBNL RFQ output beams and with the LANL RFQ output beams are given in Appendix A and Appendix B, respectively.

Since the with-errors RFQ output beams are systematically different from the no-errors RFQ output beams, it might be argued that the average with-errors beam parameters should have been used when establishing the settings of the first four quadrupoles. One would then have to create an RFQ output beam with the average properties to do the optimization of the last four quadrupoles and last cavity. It might be worth the effort at some time in the future to check if this makes a difference in the performance of the machines.

A 16-mrad chopper deflection moves the beam centroid at the chopper stopper by 0.968 cm. The undeflected and the fully deflected LBNL no-errors beam (that has gone through a MEBT without errors) are shown in Figure 3, top. The same is shown in Figure 3, bottom, for the case-7 beam with the case-7 MEBT errors. Clearly, in order to stop all fully deflected beam, some particles of the undeflected beam need to also be stopped. Put differently, if one does not routinely want to stop some fraction of the beam, one might want to be able to deflect the beam more than 16 mrad with the chopper and antichopper. Then it might be necessary to have quadrupoles between the chopper and antichopper with bore radii of more than 2.0 cm.

Error Limits

At LANL, we specify error limits e and assume errors that are uniformly distributed between $-e$ and $+e$. The PARMILA input decks of Appendix A and Appendix B show the error limits we used in the simulations.

The error limits were arrived at in consultation with John Staples, who assumes Gaussian-distributed errors and quotes rms values. For instance, John assumes quadrupole-gradient errors with 1.0% rms. This corresponds to an error limit of 1.732%. For quadrupole misalignments, John distinguishes between the misalignment of a support structure and the misalignment of the quadrupole relative to the support structure, with 1.5 mil and 1.0 mil rms values, respectively. He advised us to add these two errors in quadrature, thus resulting in about a 1.8-mil rms error and 3.122-mil error limit.

John considers cavity errors and finds them to have a negligible effect. We can not treat these errors in transport lines, but this does not seem to be a problem here.

John does not consider quadrupole-tilt and quadrupole-roll errors. Therefore, we used the same limits as elsewhere in the machine.

Machine Performance

The ten with-errors RFQ output beams were transported through the machines with ten sets of errors. The same ten sets of errors were used for the two sets of beams. Since the focus is different for the two MEBTs, the quadrupoles have the same fractional errors but not the same absolute values.

All losses in the MEBT occur at the downstream end of the antichopper. At this point, the alignment errors have accumulated, the beam size is large, vertically, and the aperture is small. The losses for the ten with-errors runs amount to 0, 0, 0, 4, 0, 7, 0, 0, 9, 1 particles for the LBNL beams and 0, 0, 2, 5, 2, 9, 10, 0, 19, 10, 0 particles for the LANL beams. These MEBT losses can easily be avoided by some steering through the restricting aperture. They can also be avoided by focusing the beam somewhat larger, vertically, at the chopper stopper. This will result in a smaller vertical beam size at the antichopper. However, the separation between the unchopped beam and the chopped beam may become marginal.

For the LANL beams, there were no further losses. For the LBNL beams, one particle was lost in the DTL in case 5 and six in case 7. A 134.8-MeV particle was lost in section 115 of the CCL in case 3, and a 19.9-MeV particle was lost in section 3 of the CCDTL in case 9.

Figures 4 through 6 represent the LBNL beams and Figures 7 through 9 represent the LANL beams. The rms emittances are shown in the top plots and the beam extents are

shown in the bottom plots. Figures 4 and 7 show the beam in the MEBT, Figures 5 and 8 show the beam in the DTL, and Figures 6 and 9 show the beam in the CCDTL and CCL.

For the CCL output beams, the following statements can be made. The transverse rms emittances of the LBNL beams range between $0.348 \pi\text{-mm-mrad}$ and $0.417 \pi\text{-mm-mrad}$, with one beam having a much larger value of $0.488 \pi\text{-mm-mrad}$. The longitudinal rms emittances range between $0.479 \pi\text{-mm-mrad}$ and $0.680 \pi\text{-mm-mrad}$. The transverse rms emittances of the LANL beams range between $0.305 \pi\text{-mm-mrad}$ and $0.377 \pi\text{-mm-mrad}$, with one beam having a value of $0.440 \pi\text{-mm-mrad}$. The longitudinal rms emittances range between $0.488 \pi\text{-mm-mrad}$ and $0.649 \pi\text{-mm-mrad}$. The LANL CCL output beams thus have about 10% smaller transverse rms emittances than the LBNL beams. Of course, the LANL RFQ output beams also have smaller transverse rms emittances, namely by about 15%.

Summary

We have documented a MEBT focus that had been obtained with the LBNL no-errors RFQ output beam and another MEBT focus that had been obtained with the LANL no-errors RFQ output beam. These foci were used when tracking the sets of with-errors RFQ output beams through the MEBT, DTL, CCDTL and CCL. Both sets of runs showed losses at the downstream end of the antichopper. Such losses can be avoided with a different focus in the MEBT, one that may or may not leave enough clearance between the undeflected and deflected beams at the chopper stopper.

Additionally, there were some losses in the DTL, CCDTL and CCL for the LBNL beams. This was at least partly due to the fact that the LBNL RFQ output beams had a larger range of energies and wider spread of phases than the LANL beams. The bunching cavities thus had a more adverse effect on the LBNL beams than on the LANL beams. In actuality, the RFQ would presumably be adjusted to produce the correct beam energy and the bunching cavities would be correctly phased for the beam from the RFQ, so that the MEBT will probably not have as big of an effect on the beam as suggested by the simulations.

The LBNL RFQ output beams had larger transverse rms emittances than the LANL beams and thus the CCL output beams had larger rms emittances as well. The transverse rms emittances of all 20 CCL output beams stayed below the canonical value of $0.500 \pi\text{-mm-mrad}$ required by the accumulator ring.

Obviously, other combinations of the settings of the first four quadrupoles, and the last four quadrupoles and last cavity, are possible that might result in beams with better properties. There also are different sets of settings allowed for the center section of the MEBT. To optimize the MEBT would be a study in itself. This memo was mainly intended to document the new MEBT geometry and the settings used for the error studies.

References

- [1] Barbara Blind and Robert Garnett, “Discussion of 14-Quadrupole SNS MEBT”, LANSCE-1:99-063, April 8, 1999.

Table 1. RFQ input-beam current, number of macroparticles transmitted through RFQ and RFQ output-beam current for LBNL beams. Case 0 is the no-errors case and cases 1 through 10 are the ten with-errors cases. The average of cases 1 through 10 is also given.

case number	input-beam current [mA]	number of macroparticles out	output-beam current [mA]
0	60.0	9160	54.960
1	59.7	9152	54.637
2	60.5	8698	52.623
3	59.0	8251	48.681
4	58.4	8809	51.445
5	60.5	8496	51.401
6	62.8	8434	52.966
7	58.7	8019	47.072
8	61.3	8950	54.864
9	61.3	8475	51.952
10	61.8	8792	54.335
$\langle 1-10 \rangle$			51.9976

Table 2. Twiss parameters of LBNL RFQ output beams after 90° roll. Case 0 is the no-errors case and cases 1 through 10 are the ten with-errors cases. The average of cases 1 through 10 is also given.

case number	α_x	β_x [m]	α_y	β_y [m]	α_z	β_z [°/keV]
0	-1.607	0.16012	1.983	0.19556	0.130	1.2828
1	-1.577	0.15665	1.942	0.19229	0.128	1.1949
2	-1.512	0.14898	1.890	0.18855	0.038	1.0611
3	-1.562	0.15137	1.825	0.17874	0.247	1.1718
4	-1.537	0.15129	1.859	0.18560	-0.045	1.0930
5	-1.548	0.15086	1.859	0.18754	-0.256	1.0322
6	-1.550	0.15245	1.824	0.18086	0.117	1.1218
7	-1.464	0.14226	1.762	0.17901	-0.408	0.9837
8	-1.581	0.15686	1.921	0.19051	0.094	1.1939
9	-1.594	0.15732	1.864	0.18406	0.190	1.2351
10	-1.564	0.15633	1.876	0.18758	-0.054	1.1531
$\langle 1-10 \rangle$	-1.5489	0.152437	1.8622	0.185474	0.0051	1.12406

Table 3. Rms emittances of LBNL RFQ output beams after 90° roll. Case 0 is no-errors case and cases 1 through 10 are ten with-errors cases. The average of cases 1 through 10 is also given.

case number	ϵ_x [π -mm-mrad]	ϵ_y [π -mm-mrad]	ϵ_z [π -°-keV]
0	0.204	0.206	106.8
1	0.210	0.214	110.1
2	0.236	0.230	114.3
3	0.236	0.241	118.1
4	0.227	0.226	112.1
5	0.221	0.222	119.1
6	0.233	0.235	117.1
7	0.235	0.237	129.1
8	0.217	0.220	112.6
9	0.218	0.219	113.8
10	0.217	0.218	112.2
$\langle 1-10 \rangle$	0.2250	0.2262	115.85

Table 4. Phase and energy description of the LBNL RFQ output beams after 90° roll. Case 0 is the no-errors case and cases 1 through 10 are the ten with-errors cases.

case number	Φ_{ave} [°]	Φ_{min} [°]	Φ_{max} [°]	E_{ave} [MeV]	E_{min} [MeV]	E_{max} [MeV]
0	1.368	-25.877	40.777	2.507	2.470	2.551
1	-0.001	-24.903	39.870	2.506	2.456	2.549
2	-1.123	-27.526	35.193	2.509	2.457	2.554
3	4.144	-24.360	42.511	2.503	2.452	2.551
4	0.101	-25.211	51.659	2.512	2.472	2.563
5	-0.846	-24.642	70.867	2.517	2.467	2.565
6	0.755	-25.514	39.493	2.506	2.459	2.548
7	-1.022	-24.242	85.473	2.522	2.423	2.569
8	0.673	-27.316	39.223	2.507	2.461	2.555
9	3.114	-25.145	40.353	2.505	2.460	2.550
10	0.472	-25.123	50.646	2.511	2.472	2.559

Table 5. Number of macroparticles transmitted through the RFQs and output-beam current for the LANL RFQ output beams. Case 0 is the no-errors case and cases 1 through 10 are the ten with-errors cases. The average of cases 1 through 10 is also given.

case number	number of macroparticles out	output-beam current [mA]
0	9375	56.250
1	9269	55.614
2	9442	56.652
3	9354	56.124
4	9395	56.370
5	9415	56.490
6	9536	57.216
7	9488	56.928
8	9394	56.364
9	9288	55.728
10	9408	56.448
$\langle 1-10 \rangle$		56.3994

Table 6. Twiss parameters of the LANL RFQ output beams after 90° roll. Case 0 is the no-errors case and cases 1 through 10 are the ten with-errors cases. The average of cases 1 through 10 is also given.

case number	α_x	β_x [m]	α_y	β_y [m]	α_z	β_z [°/keV]
0	-2.385	0.21317	1.924	0.16708	-0.170	1.2375
1	-2.363	0.20648	1.940	0.16418	-0.154	1.1453
2	-2.351	0.21536	1.897	0.16472	-0.145	1.3145
3	-2.325	0.20637	1.908	0.16293	-0.148	1.1897
4	-2.344	0.20823	1.894	0.16280	-0.149	1.2108
5	-2.342	0.20283	1.890	0.15892	-0.175	1.1130
6	-2.389	0.20574	1.891	0.15951	-0.171	1.1210
7	-2.372	0.20405	1.898	0.16011	-0.211	1.1317
8	-2.348	0.20337	1.949	0.16332	-0.142	1.1343
9	-2.394	0.20713	1.930	0.16147	-0.159	1.1363
10	-2.373	0.20113	1.901	0.15729	-0.168	1.0963
$\langle 1-10 \rangle$	-2.3601	0.206069	1.9098	0.161525	-0.1622	1.1593

Table 7. Rms emittances for the LANL RFQ output beams after 90° roll. Case 0 is the no-errors case and cases 1 through 10 are the ten with-errors cases. The average of cases 1 through 10 is also given.

case number	ϵ_x [π -mm-mrad]	ϵ_y [π -mm-mrad]	ϵ_z [π -°-keV]
0	0.187	0.185	104.6
1	0.190	0.188	107.6
2	0.187	0.187	107.2
3	0.190	0.191	106.6
4	0.193	0.191	107.6
5	0.196	0.196	107.6
6	0.186	0.190	103.3
7	0.189	0.190	104.8
8	0.186	0.189	103.1
9	0.187	0.186	102.3
10	0.190	0.190	105.6
$\langle 1-10 \rangle$	0.1894	0.1898	105.57

Table 8. Phase and energy description of the LANL RFQ output beams after 90° roll. Case 0 is the no-errors case and cases 1 through 10 are the ten with-errors cases.

case number	Φ_{ave} [°]	Φ_{min} [°]	Φ_{max} [°]	E_{ave} [MeV]	E_{min} [MeV]	E_{min} [MeV]
0	-28.811	-55.255	6.199	2.507	2.464	2.555
1	-30.459	-55.756	1.530	2.496	2.452	2.537
2	-26.977	-56.553	8.888	2.496	2.460	2.541
3	-29.322	-53.822	6.683	2.496	2.449	2.562
4	-28.948	-55.013	7.068	2.495	2.445	2.555
5	-31.570	-54.123	-1.248	2.494	2.449	2.544
6	-32.765	-57.051	-2.614	2.493	2.446	2.534
7	-32.012	-57.850	2.933	2.494	2.439	2.538
8	-31.861	-55.604	1.633	2.495	2.456	2.549
9	-31.844	-56.836	-2.344	2.496	2.447	2.549
10	-32.780	-56.850	-1.804	2.495	2.446	2.544

Appendix A. PARMILA input deck for simulating latest 14-quadrupole MEBT tuned for LBNL no-errors RFQ output beam.

```

comment compile with -25 limit
run 1 1
title
Neuschaefer SNS 1Tank, bore r=1.25/1.5cm, Ep=1.3Ek, -45deg,Q1=3.5&3.90to2.95
charge -1
linac 1 2.5 402.5 1.001089
current 36
tank 1 -84 -45.0 0.030753 0.000 0.043 0 0. 3. -3.
      3.5 2 4 11 0. 1.25 1.50 42. 0. 0 0 0 0 0 0 0 0 1 1
comment; Include this file in the PARMILA input file.
comment; Shunt impedance Z reduced by user-supplied factor = 0.8000.
comment; Geometric beta column not included.
sfdata
comment; Bore = 1.25-1.50, DTL
comment; Beta T TP S SP g/bl Z
E/E0 Tave dZctr
0.070000 0.563010 0.099403 0.572469 0.022447 0.170421 49.8612
0.080000 0.630698 0.088647 0.547776 0.032845 0.162626 51.9943
0.090000 0.682070 0.079703 0.524643 0.039624 0.159948 53.8256
0.100000 0.722067 0.072120 0.503294 0.043986 0.160757 55.3527
0.110000 0.756748 0.064987 0.480954 0.046806 0.156429 56.7438
0.120000 0.782850 0.059350 0.462490 0.048490 0.157125 57.8702
0.130000 0.802303 0.055025 0.447951 0.049549 0.161141 58.8976
0.132500 0.802039 0.055054 0.447798 0.049451 0.158835 59.2262
0.135000 0.801363 0.055190 0.448117 0.049371 0.157402 59.5494
0.137500 0.800316 0.055419 0.448850 0.049302 0.156749 59.8646
0.140000 0.799115 0.055689 0.449827 0.049250 0.156805 60.1312
0.142500 0.797525 0.056061 0.451207 0.049210 0.157405 60.4238
0.145000 0.795716 0.056488 0.452832 0.049178 0.158524 60.7050
0.147500 0.793722 0.056967 0.454697 0.049160 0.160095 60.9725
0.150000 0.791518 0.057493 0.456748 0.049138 0.162078 61.2272
0.160000 0.807049 0.053959 0.444589 0.049834 0.164969 61.9518
0.170000 0.820006 0.050932 0.433903 0.050274 0.167814 62.6357
0.180000 0.830799 0.048358 0.424649 0.050548 0.170608 63.3001
0.190000 0.839863 0.046156 0.416668 0.050716 0.173421 63.9490
0.200000 0.847380 0.044307 0.409988 0.050831 0.176304 64.6292
0.210000 0.853438 0.042809 0.404710 0.050941 0.179423 65.3802 -1
change 10 6700. 1 300 1
change 14 2.49 6700.0 20.1 4600.
change 3
error 3.122 .57 3.122 .57 .5 .005 .001 .01732 0 .25
linout
linout 4
elimit 1.00
comment input -8 10000 -.268 56.3 .0018 -.136 17.5 .0018 .0799 25.3 .00272
scheff 0 0.05 0.05 20 40 0 0 1 1 2
adjust -46.37 0
comment change 6 2 0
start 0
stop 0
transl 1 1 0.0e-1 1 1.5 0 1 1
transl 2 1 10.0 4 1.5 0 1 1
transl 3 3 -2135.778 7.0 1.5 1 1 1
transl 4 1 7.5 2 1.5 0 1 1
transl 5 3 3057.734 7.0 1.5 1 1 1
transl 6 1 6.0 2 1.5 0 1 1
transl 7 3 -2679.749 7.0 1.5 1 1 1
transl 8 1 7.5 2 1.5 0 1 1
transl 9 2 0.075 -90. 1 1.5 0 0
transl 10 1 7.5 2 1.5 0 1 1
transl 11 3 1469.043 7.0 1.5 1 1 1
transl 12 1 11.0 4 1.5 0 1 1
transl 13 7 1.5 0.9

```

```

transl 14 1 17.5 10 1.5 0 1 1
transl 15 7 1.5 0.9
transl 16 20 0.0 0.0 0.0 0.0
transl 17 1 17.5 10 1.5 0 1 1
transl 18 7 1.5 1.05 -1.5 -0.75
transl 19 1 15.5 5 2.0 0 1 1
transl 20 2 0.049 -90. 1 1.5 0 0
transl 21 1 7.5 2 2.0 0 1 1
transl 22 3 -1600.0 7.0 2.0 1 1 1
transl 23 1 3.0 2 2.0 0 1 1
transl 24 3 2483.537 7.0 2.0 1 1 1
transl 25 1 3.0 2 2.0 0 1 1
transl 26 3 -1100.0 7.0 2.0 1 1 1
transl 27 1 13.5 4 2.0 0 1 1
transl 28 7 2.0 2.0
transl 29 1 13.5 4 2.0 0 1 1
transl 30 3 -1100.0 7.0 2.0 1 1 1
transl 31 1 3.0 2 2.0 0 1 1
transl 32 3 2483.537 7.0 2.0 1 1 1
transl 33 1 3.0 2 2.0 0 1 1
transl 34 3 -1600.0 7.0 2.0 1 1 1
transl 35 1 7.5 2 2.0 0 1 1
transl 36 2 0.049 -90. 1 1.5 0 0
transl 37 1 15.5 5 2.0 0 1 1
transl 38 7 1.5 1.05 -1.5 -0.75
transl 39 1 17.5 10 1.5 0 1 1
transl 40 7 1.5 0.9
transl 41 20 0.0 0.0 0.0 0.0
transl 42 1 17.5 10 1.5 0 1 1
transl 43 7 1.5 0.9
transl 44 1 11.5 4 1.5 0 1 1
transl 45 3 1424.3710 7.0 1.5 1 1 1
transl 46 1 7.5 2 1.5 0 1 1
transl 47 3 -2870.6674 7.0 1.5 1 1 1
transl 48 1 7.0 2 1.5 0 1 1
transl 49 2 0.1204561 -90. 1 1.5 0 0
transl 50 1 7.0 2 1.5 0 1 1
transl 51 3 2974.6358 7.0 1.5 1 1 1
transl 52 1 7.5 2 1.5 0 1 1
transl 53 3 -3452.5325 7.0 1.5 1 1 1
transl 54 1 19.0 5 1.5 0 1 1
transl 55 19 0 0
transl 56 3 -6700.0 1.75 1.25 0 1 1
trans2 1 3 -5263.6 1.475 1.5 0 1 1
output 2 1 1 0 0 0 1 300 1
output 3 1 1 0 0 0 1
output 4 1 1 0 0 0 1
begin
end

```

Appendix B. PARMILA input deck for simulating latest 14-quadrupole MEBT tuned for LANL no-errors RFQ output beam.

```

comment compile with -25 limit
run 1 1
title
Neuschaefer SNS 1Tank, bore r=1.25/1.5cm, Ep=1.3Ek, -45deg,Q1=3.5&3.90to2.95
charge -1
linac 1 2.5 402.5 1.001089
current 36
tank 1 -84 -45.0 0.030753 0.000 0.043 0 0. 3. -3.
      3.5 2 4 11 0. 1.25 1.50 42. 0. 0 0 0 0 0 0 0 0 1 1
comment; Include this file in the PARMILA input file.
comment; Shunt impedance Z reduced by user-supplied factor = 0.8000.
comment; Geometric beta column not included.
sfdata
comment; Bore = 1.25-1.50, DTL
comment; Beta T TP S SP g/bl Z
E/E0 Tave dZctr
0.070000 0.563010 0.099403 0.572469 0.022447 0.170421 49.8612
0.080000 0.630698 0.088647 0.547776 0.032845 0.162626 51.9943
0.090000 0.682070 0.079703 0.524643 0.039624 0.159948 53.8256
0.100000 0.722067 0.072120 0.503294 0.043986 0.160757 55.3527
0.110000 0.756748 0.064987 0.480954 0.046806 0.156429 56.7438
0.120000 0.782850 0.059350 0.462490 0.048490 0.157125 57.8702
0.130000 0.802303 0.055025 0.447951 0.049549 0.161141 58.8976
0.132500 0.802039 0.055054 0.447798 0.049451 0.158835 59.2262
0.135000 0.801363 0.055190 0.448117 0.049371 0.157402 59.5494
0.137500 0.800316 0.055419 0.448850 0.049302 0.156749 59.8646
0.140000 0.799115 0.055689 0.449827 0.049250 0.156805 60.1312
0.142500 0.797525 0.056061 0.451207 0.049210 0.157405 60.4238
0.145000 0.795716 0.056488 0.452832 0.049178 0.158524 60.7050
0.147500 0.793722 0.056967 0.454697 0.049160 0.160095 60.9725
0.150000 0.791518 0.057493 0.456748 0.049138 0.162078 61.2272
0.160000 0.807049 0.053959 0.444589 0.049834 0.164969 61.9518
0.170000 0.820006 0.050932 0.433903 0.050274 0.167814 62.6357
0.180000 0.830799 0.048358 0.424649 0.050548 0.170608 63.3001
0.190000 0.839863 0.046156 0.416668 0.050716 0.173421 63.9490
0.200000 0.847380 0.044307 0.409988 0.050831 0.176304 64.6292
0.210000 0.853438 0.042809 0.404710 0.050941 0.179423 65.3802 -1
change 10 6700. 1 300 1
change 14 2.49 6700.0 20.1 4600.
change 3
error 3.122 .57 3.122 .57 .5 .005 .001 .01732 0 .25
linout
linout 4
elimit 1.00
comment input -8 10000 -.268 56.3 .0018 -.136 17.5 .0018 .0799 25.3 .00272
scheff 0 0.05 0.05 20 40 0 0 1 1 2
adjust -16.2 0
comment change 6 2 0
start 0
stop 0
transl 1 1 0.0e-1 1 1.5 0 1 1
transl 2 1 10.0 4 1.5 0 1 1
transl 3 3 -2145.808 7.0 1.5 1 1 1
transl 4 1 7.5 2 1.5 0 1 1
transl 5 3 3046.488 7.0 1.5 1 1 1
transl 6 1 6.0 2 1.5 0 1 1
transl 7 3 -2650.091 7.0 1.5 1 1 1
transl 8 1 7.5 2 1.5 0 1 1
transl 9 2 0.075 -90. 1 1.5 0 0
transl 10 1 7.5 2 1.5 0 1 1
transl 11 3 1443.293 7.0 1.5 1 1 1
transl 12 1 11.0 4 1.5 0 1 1
transl 13 7 1.5 0.9

```

```

transl 14 1 17.5 10 1.5 0 1 1
transl 15 7 1.5 0.9
transl 16 20 0.0 0.0 0.0 0.0
transl 17 1 17.5 10 1.5 0 1 1
transl 18 7 1.5 1.05 -1.5 -0.75
transl 19 1 15.5 5 2.0 0 1 1
transl 20 2 0.049 -90. 1 1.5 0 0
transl 21 1 7.5 2 2.0 0 1 1
transl 22 3 -1600.0 7.0 2.0 1 1 1
transl 23 1 3.0 2 2.0 0 1 1
transl 24 3 2483.537 7.0 2.0 1 1 1
transl 25 1 3.0 2 2.0 0 1 1
transl 26 3 -1100.0 7.0 2.0 1 1 1
transl 27 1 13.5 4 2.0 0 1 1
transl 28 7 2.0 2.0
transl 29 1 13.5 4 2.0 0 1 1
transl 30 3 -1100.0 7.0 2.0 1 1 1
transl 31 1 3.0 2 2.0 0 1 1
transl 32 3 2483.537 7.0 2.0 1 1 1
transl 33 1 3.0 2 2.0 0 1 1
transl 34 3 -1600.0 7.0 2.0 1 1 1
transl 35 1 7.5 2 2.0 0 1 1
transl 36 2 0.049 -90. 1 1.5 0 0
transl 37 1 15.5 5 2.0 0 1 1
transl 38 7 1.5 1.05 -1.5 -0.75
transl 39 1 17.5 10 1.5 0 1 1
transl 40 7 1.5 0.9
transl 41 20 0.0 0.0 0.0 0.0
transl 42 1 17.5 10 1.5 0 1 1
transl 43 7 1.5 0.9
transl 44 1 11.5 4 1.5 0 1 1
transl 45 3 1419.8094 7.0 1.5 1 1 1
transl 46 1 7.5 2 1.5 0 1 1
transl 47 3 -2863.2952 7.0 1.5 1 1 1
transl 48 1 7.0 2 1.5 0 1 1
transl 49 2 0.1176 -90. 1 1.5 0 0
transl 50 1 7.0 2 1.5 0 1 1
transl 51 3 2963.0334 7.0 1.5 1 1 1
transl 52 1 7.5 2 1.5 0 1 1
transl 53 3 -3467.8928 7.0 1.5 1 1 1
transl 54 1 19.0 5 1.5 0 1 1
transl 55 19 0 0
transl 56 3 -6700.0 1.75 1.25 0 1 1
trans2 1 3 -5263.6 1.475 1.5 0 1 1
output 2 1 1 0 0 0 1 300 1
output 3 1 1 0 0 0 1
output 4 1 1 0 0 0 1
begin
end

```

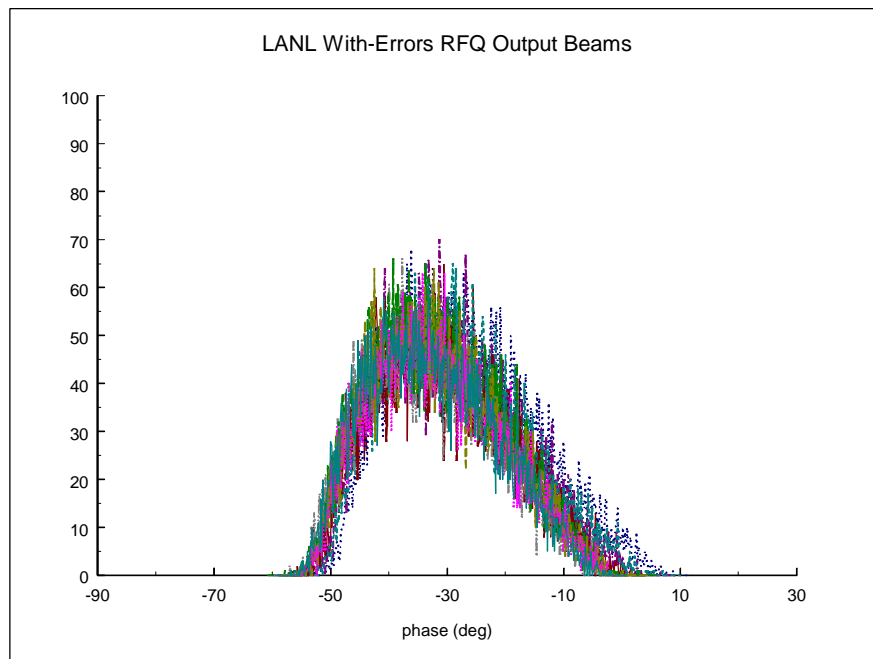
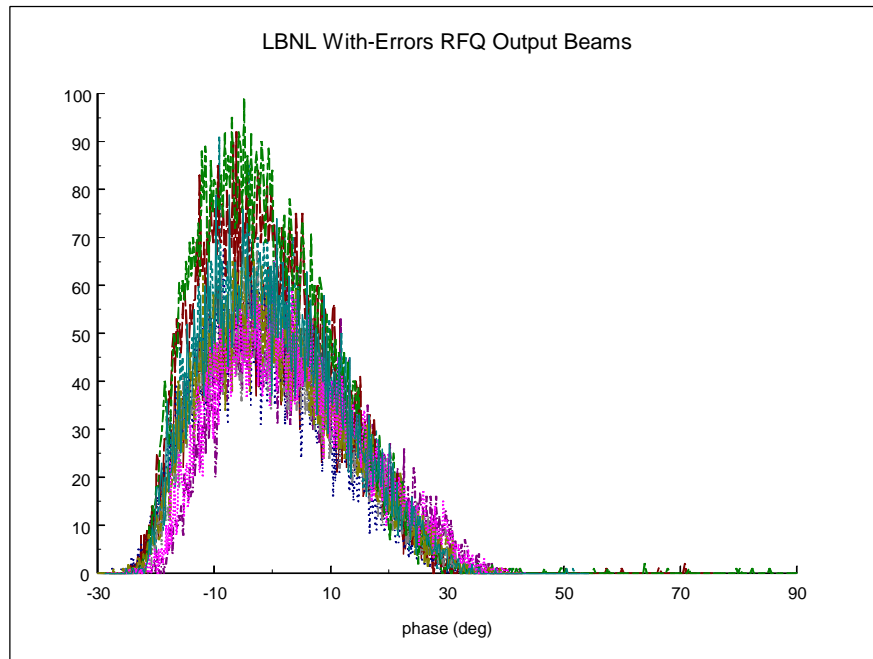


Figure 1. Phase distributions of ten LBNL with-errors RFQ output beams (top) and ten LANL with-errors RFQ output beams (bottom)

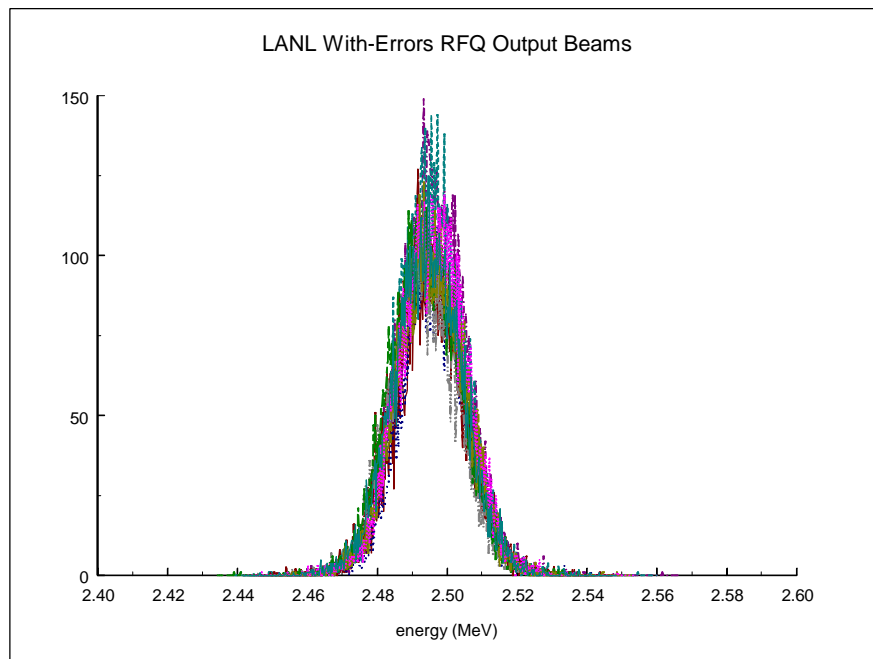
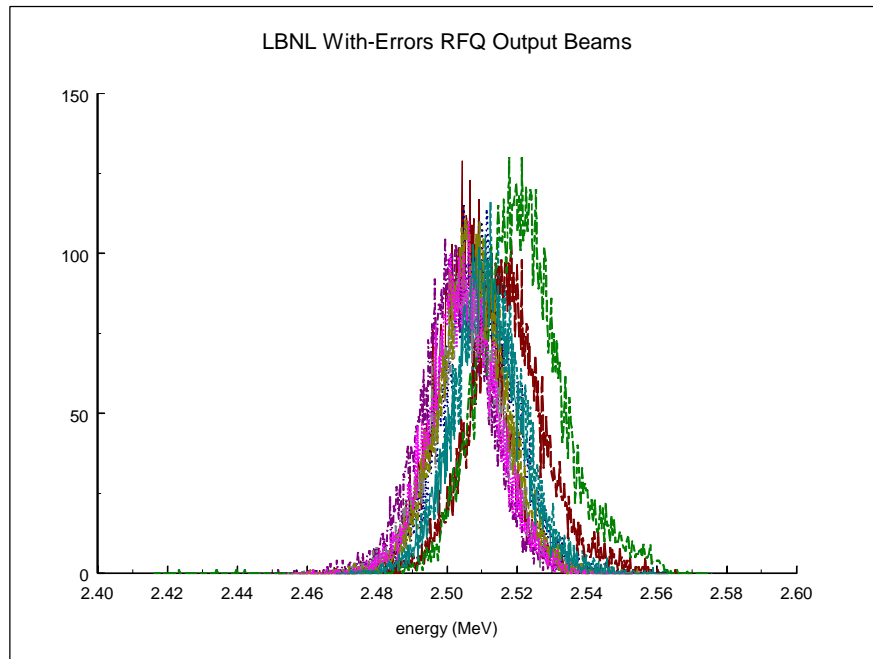


Figure 2. Energy distributions of ten LBNL with-errors RFQ output-beams (top) and ten LANL with-errors RFQ output beams (bottom).

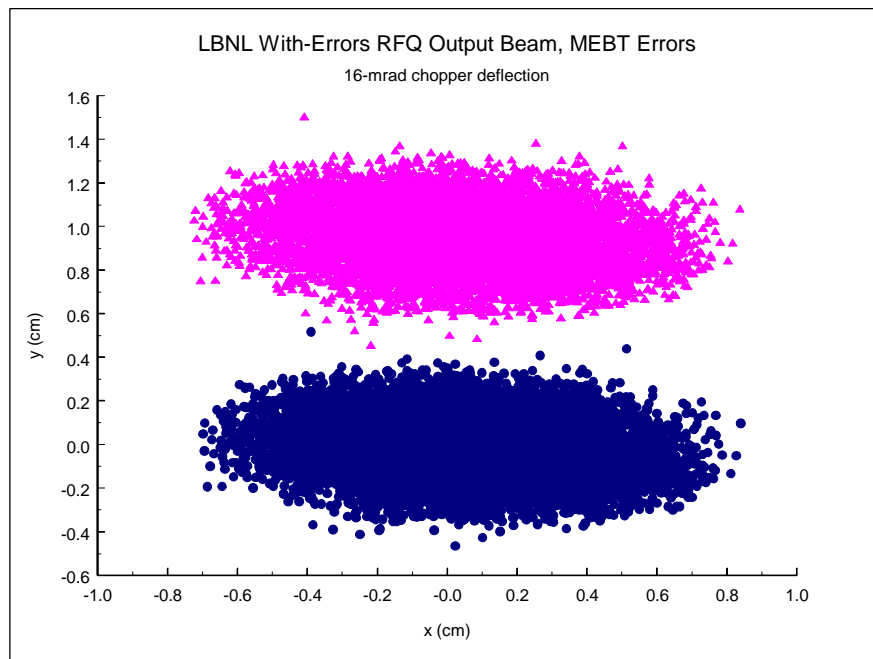
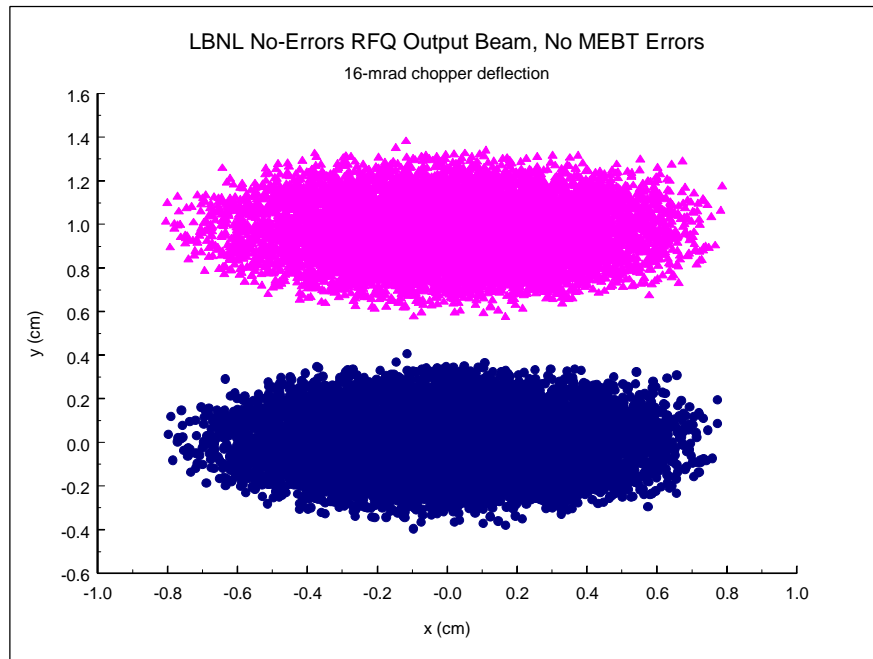


Figure 3. Footprints, at chopper stopper, of LBNL beams with 0-mrad and 16-mrad deflection. Shown are the no-errors case (top) and the with-errors case 7 (bottom).

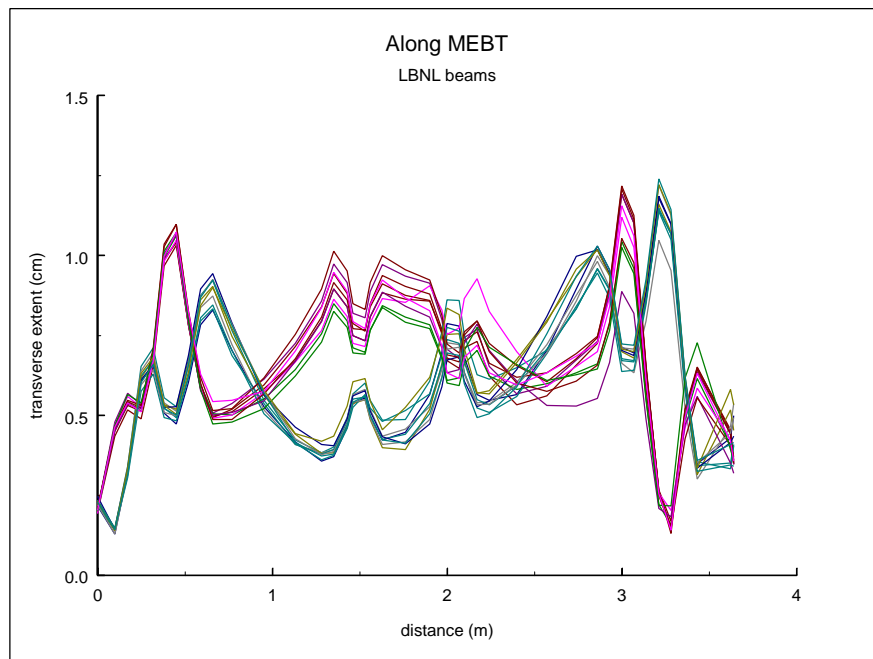
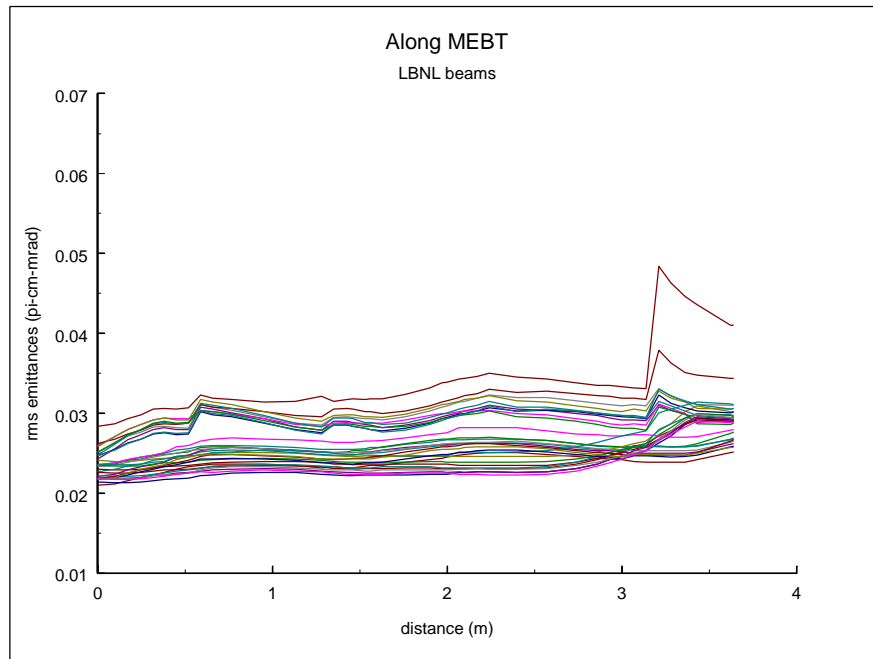


Figure 4. Transverse and longitudinal rms emittances (top) and maximum beam extents (bottom) for with-errors LBNL beams in MEBT.

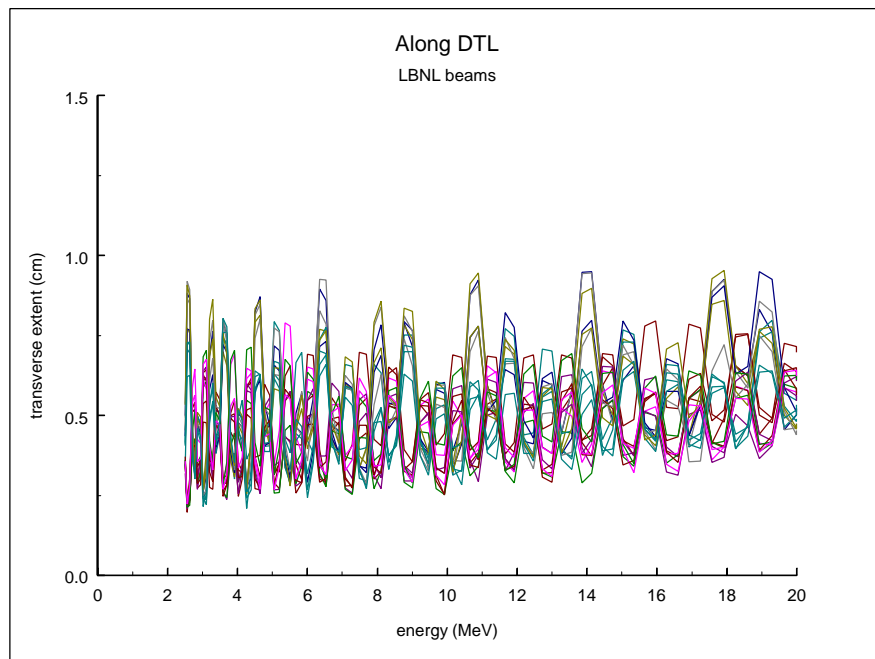
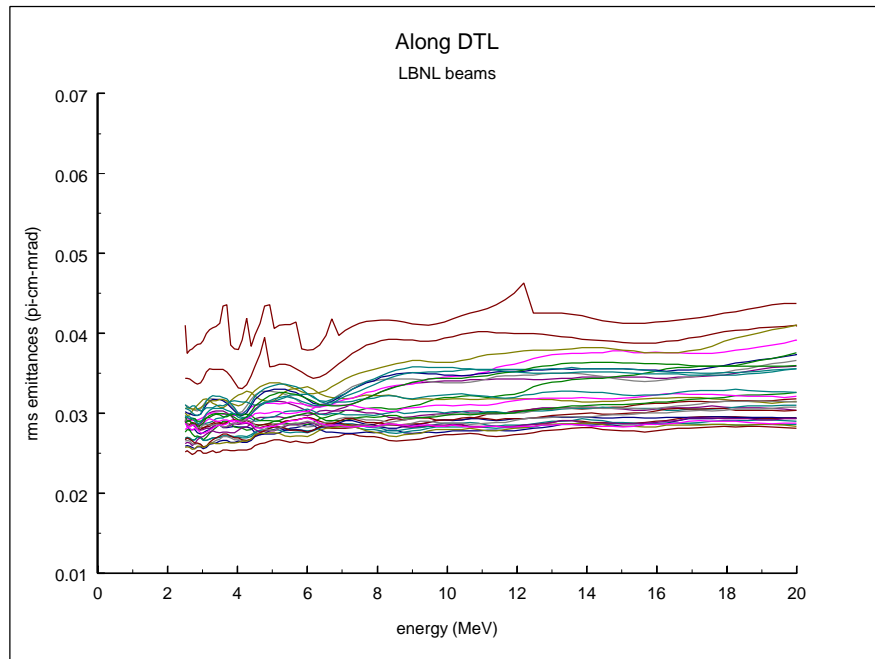


Figure 5. Transverse and longitudinal rms emittances (top) and maximum beam extents (bottom) for with-errors LBNL beams in DTL.

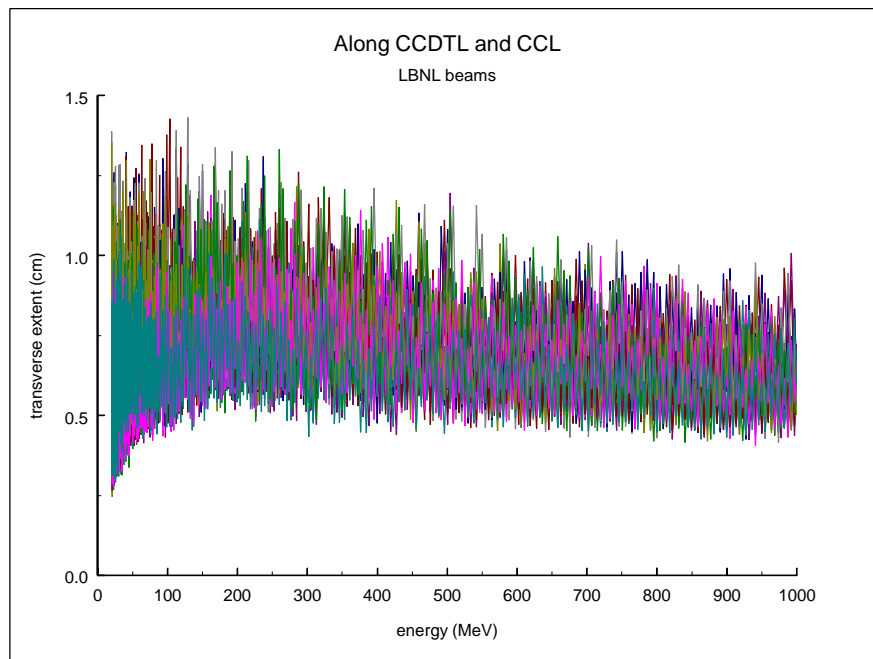
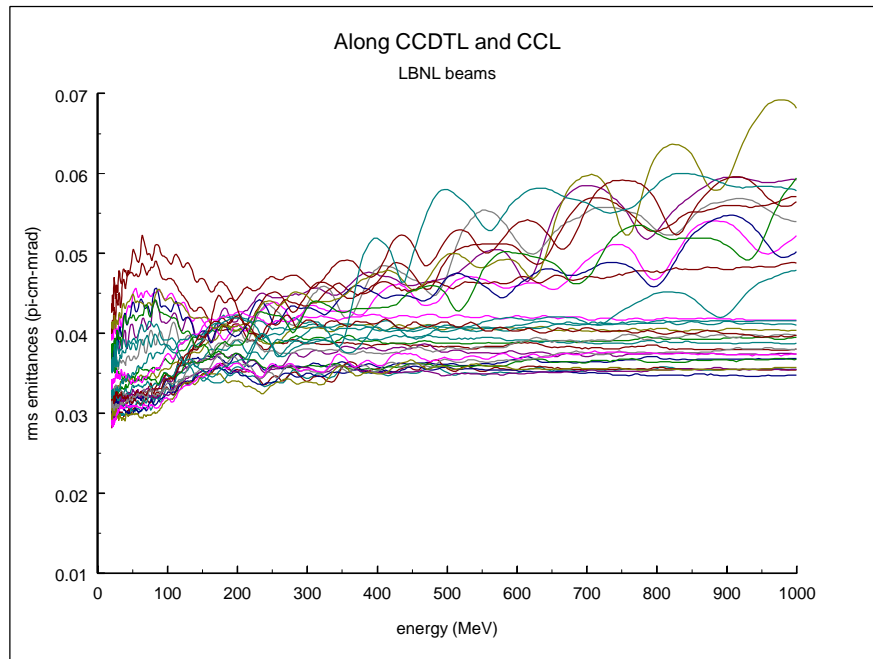


Figure 6. Transverse and longitudinal rms emittances (top) and maximum beam extents (bottom) for with-errors LBNL beams in CCDTL and CCL.

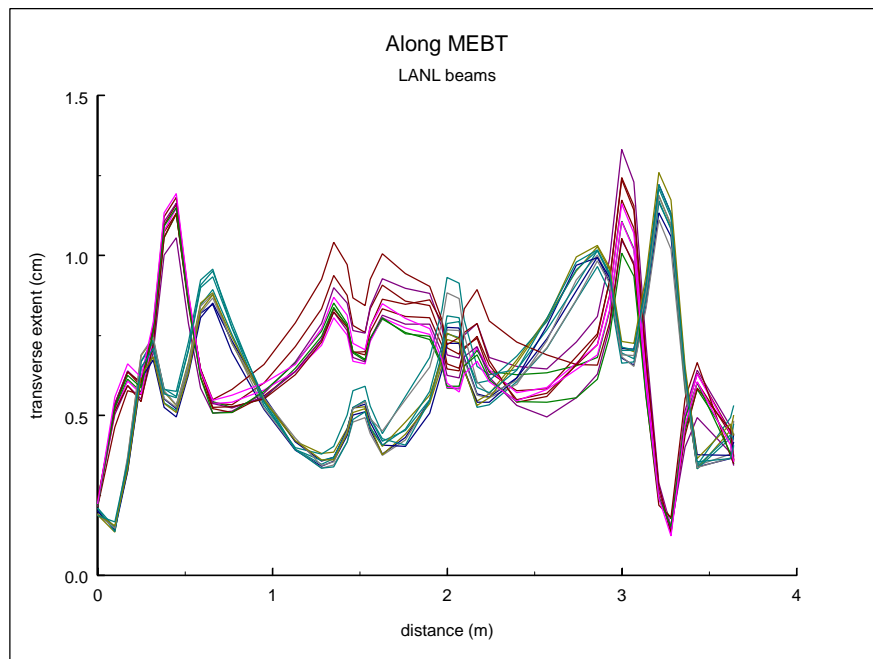
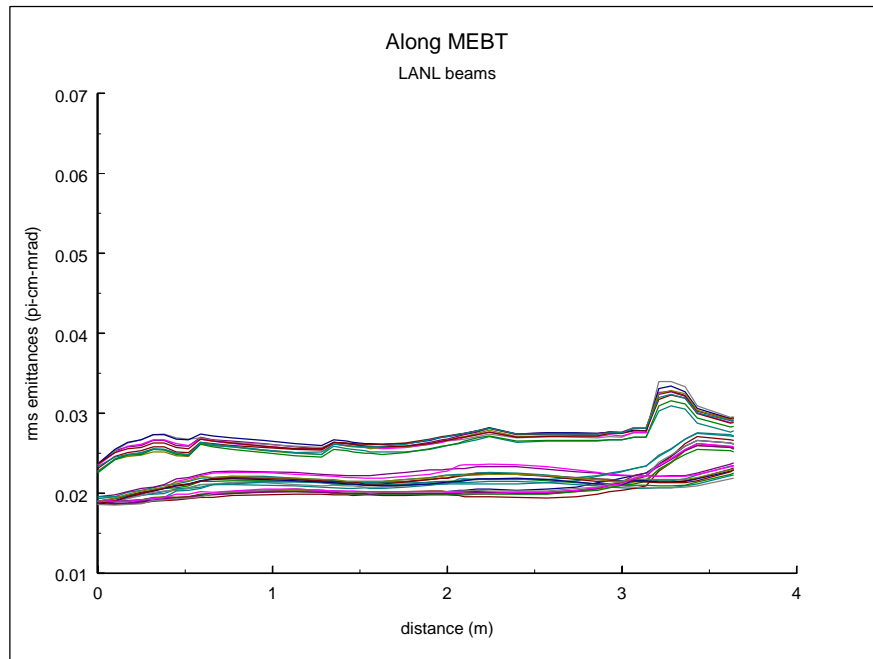


Figure 7. Transverse and longitudinal rms emittances (top) and maximum beam extents (bottom) for with-errors LANL beams in MEBT.

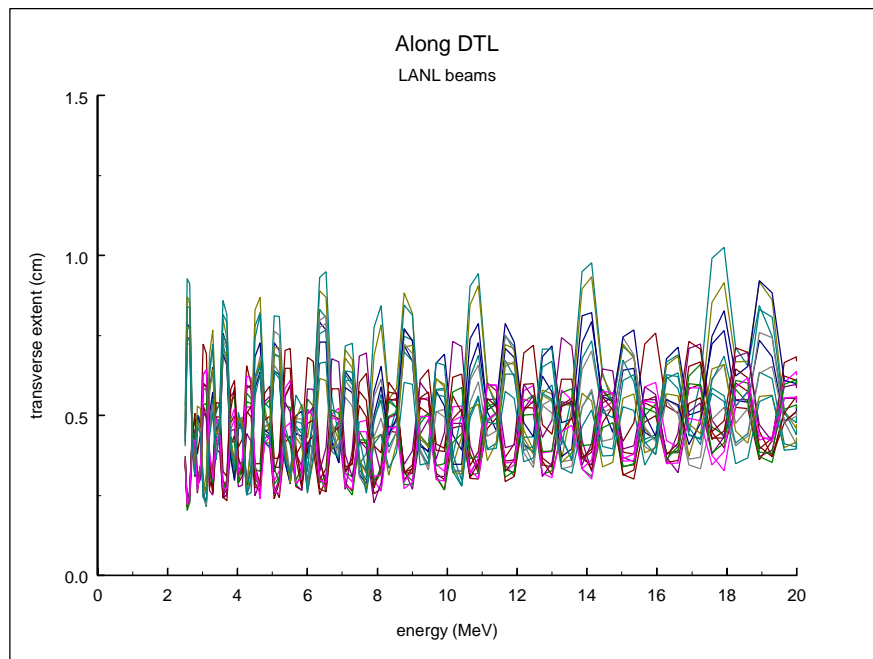
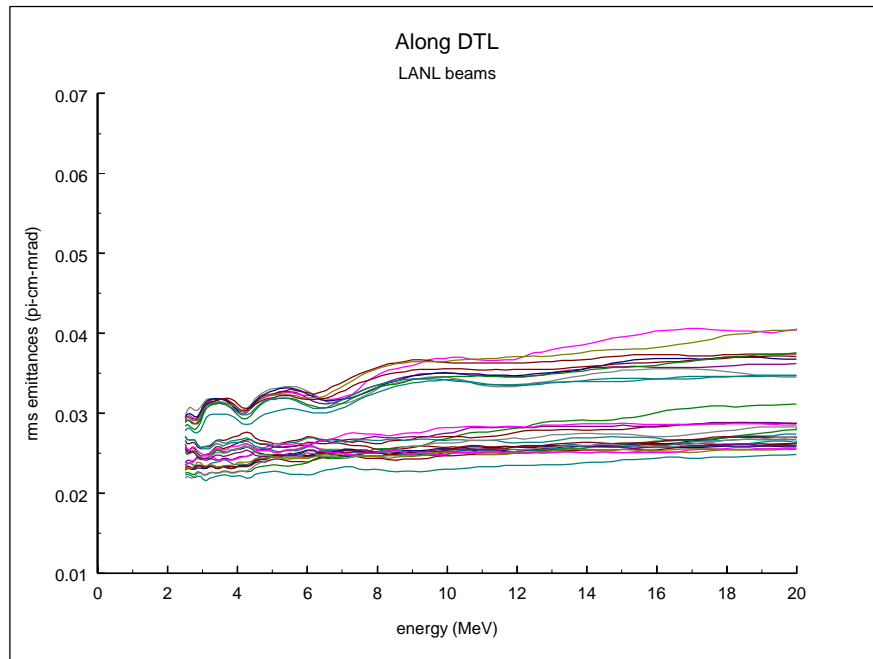


Figure 8. Transverse and longitudinal rms emittances (top) and maximum beam extents (bottom) for with-errors LANL beams in DTL.

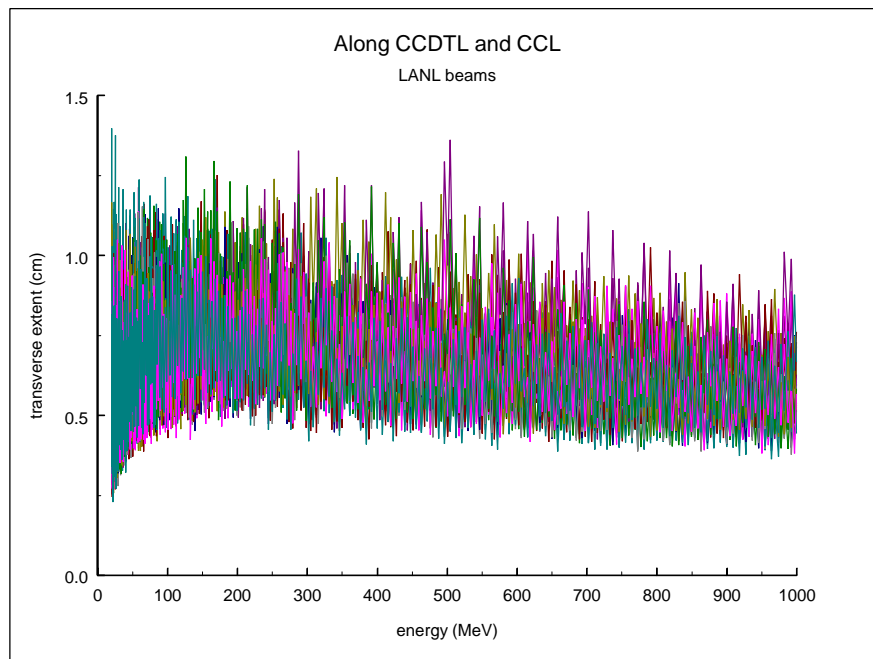
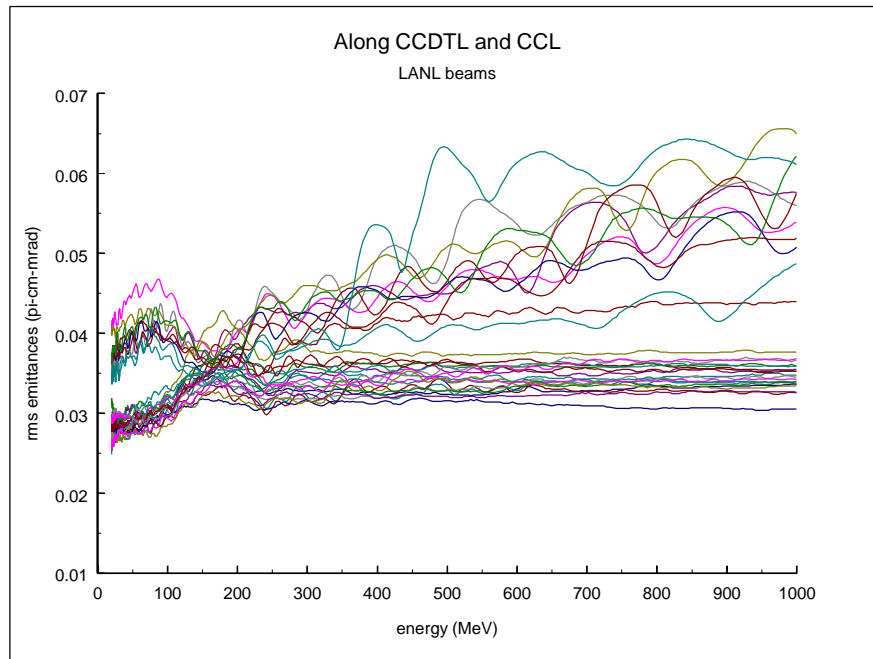


Figure 9. Transverse and longitudinal rms emittances (top) and maximum beam extents (bottom) for with-errors LANL beams in CCDTL and CCL.